WASHINGTON STATE DEPARTMENT OF
Natural Resources
Doug Sutherland - Commissioner of Public Lands
Division of Geology and Earth Resources
Ron Teissere - State Geologist

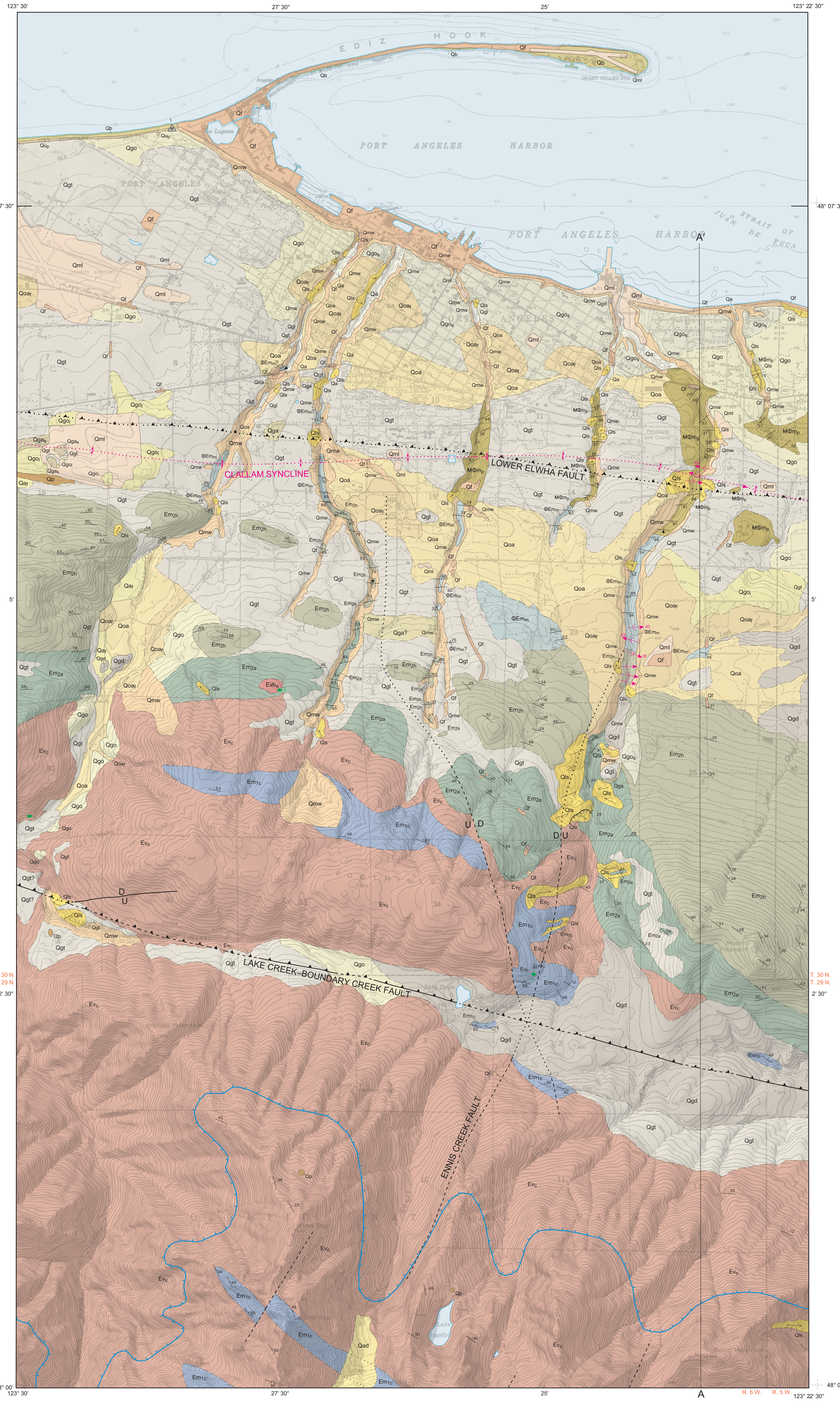

Lambert conformal conic projection
North American Datum of 1927. To place on North American Datum of 1983, move projection lines 24 meters north and 96 meters east as shown by dashed corner ticks
Base map from scanned and rectified U.S. Geological Survey 7.5-minute Port Angeles and Ediz Hook quadrangles, 1961 (photorevised 1985) and 1961 (photorevised 1978) respectively
Digital cartography by J. Eric Schuster, Sandra L. McAuliffe, and Anne C. Heinitz
Editing and production by Jaretta M. Roloff

SCALE 1:24 000
1 MILE; 7000 FEET; 1 KILOMETER
contour interval 20 feet

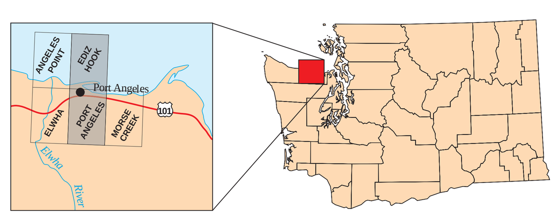

Geologic Map of the Port Angeles and Ediz Hook 7.5-minute Quadrangles, Clallam County, Washington

by Henry W. Schasse, Karl W. Wegmann, and Michael Polenz

June 2004

METHODS

This project was mapped concurrently with the Elwha and Angeles Point quadrangles, which assisted us in our interpretation of geologic structure and Quaternary units. We used a digital elevation model (DEM) based on lidar data from the Puget Sound Lidar Consortium (http://rocky2.ess.washington.edu/data/raster/lidar/index.htm) to identify landforms and map geologic contacts with a level of confidence not previously attainable in densely vegetated or inaccessible areas. We believe that contacts are within about 200 ft of their shown location. We sought to map Quaternary units where they mask the underlying units and appear to be thick enough to be of geotechnical significance, generally 5 ft or thicker. We used selected water well logs to interpret structure and subsurface geology.

We used the geologic time scale of the Correlation of Stratigraphic Units of North America (COSUNA) project of the American Association of Petroleum Geologists (Salvador, 1985), with boundary-age modifications of Montanari and others (1985). We use 'ka' to mean thousands of calendar years before A.D. 1950. We identify radiocarbon years by the term '^{14}C'. We conform data provided by other workers to the same terminology, unless we are unsure of their meaning, in which case we report their terminology in quotation marks. Some of the volcanic rocks are identified using whole-rock geochemistry and total-alkali silica diagrams (Zanettin, 1984). Sandstones are named using the classification scheme of Dickinson (1970).

GEOLOGIC SETTING

Early to middle Eocene marine basalt and sediments are overlain by middle Eocene to lower Miocene Tertiary sedimentary rocks in the map area. We follow Snavely and others (1978) in referring to the upper, middle and lower members of the Twin River Group (Twin River Formation of Brown and Gower, 1958, and Brown and others, 1960) as the Pysht, Makah, and Hoko River Formations. The Tertiary units are folded and thrust-faulted together by post-early Miocene tectonism (see cross section A–A′). Late Quaternary sediments form a discontinuous apron over the bedrock. The Quaternary sediments generally pinch out against the mountain front above 2000 ft elevation, but can be found as high as 3800 ft (Long, 1975). They thinly drape the foothills and locally thicken to several hundred feet in the coastal plain. Alpine drift is mapped as high as 4300 ft.

Sediments of Canadian Cordilleran provenance (Vancouver Island and the Coast Ranges, hereinafter termed 'northern') were deposited in the map area by the late Wisconsinan and earlier continental glaciations. Northern sediments are distinguished from Olympic Mountains-sourced (Olympic) sediments based on their lithologic constituents. Olympic sediments consist of about 90 percent lithic sandstone. The remaining 10 percent includes basalt, argillite, and low-grade metamorphosed core rocks (mostly metasedimentary). Northern sediments are readily distinguished from Olympic sediments by inclusion of high-grade metamorphic, granitic, and other crystalline rocks. Sand facies, rich in feldspar and polycrystalline quartz, tend to be better sorted, lighter in color, and more mature than Olympic sands.

CONCEPTUAL MODEL OF LATE QUATERNARY LANDSCAPE DEVELOPMENT

The modern landscape was formed primarily by the Juan de Fuca lobe (**JFL**) of the late Wisconsinan glaciation, which deposited northern-source drift over much of this quadrangle. Northern sediments are also common in older Pleistocene deposits in unit Qu$_p$. A few Olympic alpine drift deposits (unit Qad) were recognized in the map area. Recessional continental glacial outwash (unit Qgo) is only sparsely exposed in the field area, because latest Pleistocene and Holocene alluvium (unit Qoa) obscures much of the outwash. Late Wisconsinan glacial sedimentation and surface scouring destroyed pre-glacial drainage patterns, and due to the initial absence of an organized drainage network along the coastal plain, early postglacial meltwater and other runoff caused widespread deposition of low-energy sediments (units Qgo and Qoa, respectively). At the end of the glaciation, persistent glacio-isostatic crustal depression combined with eustatic sea level rise to cause rapid relative sea level rise (Fig. 1), resulting in deposition of glaciomarine drift (included with unit Qgo$_s$) to at least 130 ft above mean sea level (Dethier and others, 1995). Younger terrestrial sediments may conceal possible deposition of glaciomarine drift at higher elevations.

Sediments on the coastal plain (units Qgo and Qoa) and extensive river terraces (unit Qoa), which are perched up to about 200 ft above the modern valley floor of north-draining creeks in the map area and along the lower Elwha River a few miles to the west of the map area (Polenz and others, 2004), appear to be graded to that elevated relative sea level. The slope and elevation of these Qoa terraces relative to the slope and elevation of glaciomarine drift up to at least 130 ft above modern mean sea level (**MSL**) along the shore suggest terrace grading to a relative base level significantly above MSL. Relative sea level maximum after deglaciation (**RSLM**) in the field area was probably reached around 13.3 ka (Fig. 1), suggesting a similar age for the highest terraces of Qoa and coeval deposition of Qgo in basins in which runoff was still dominated by JFL ice meltwater.

After RSLM, crustal rebound in response to glacial unloading caused relative sea level to drop rapidly to about 200 ft below MSL (Fig. 1; Mosher and Hewitt, 2004), which triggered cutting of the steep-walled, modern valleys that are mostly limited to the unconsolidated deposits of the field area. The rate of rebound had to greatly outstrip global sea level rise and may have reached between 68 and 74 mm/yr to permit the rate of relative sea level drop, estimated by Mosher and Hewitt (2004) at ≤58 mm/yr. Multiple river terraces (unit Qoa) dot the sidewalls of the modern valleys (although most are too small to show at map scale) and are thought to record this period of incision, with higher terraces being progressively older. The lower reaches of the larger valleys have an alluvial floor that broadens toward the shore, reflecting alluvial infilling (unit Qa) of deeper post-glacial valleys (Galster, 1989; Steve Evans, Pangeo, Inc., oral commun., 2004).

Studies near the field area suggest that crustal rebound was apparently mostly completed by 10.7 ka (Fig. 1; Mosher and Hewitt, 2004, and references therein). Therefore, deposition of unit Qa as infill of the modern valley floors commenced approximately 10.7 ka and continued until sea level approximated MSL at about 6 ka (Fig. 1; Mathews and others, 1970; Clague and others, 1982; Booth, 1987; Dragovich and others, 1994; Mosher and Hewitt, 2004). Since then, the alluvial valleys near the shore have likely undergone little change.

Holocene sea level rise has been accompanied by shoreline erosion and 3000 to 5000 ft of coastal retreat in the area (Fig. 1; Galster, 1989). This coastal retreat was accompanied by a landward migration of Ediz Hook, which is built by longshore drift transport of sediment derived from the Elwha River and shoreline erosion west of Ediz Hook (Downing, 1983; Galster, 1989).

STRUCTURAL GEOLOGY

The Clallam syncline, originally mapped by Brown and others (1960) over a distance of 30 mi, crosses the northern part of the Port Angeles quadrangle. The syncline plunges eastward within the quadrangle, and to account for structural complexities reflected in the bedding attitudes exposed along Ennis Creek (cross section A–A′), must be faulted along its hinge and its south limb in the eastern part of the map area.

Two west-trending thrust faults cross the field area. One is located along the Clallam syncline where we interpret it as a series of imbricate blind thrust faults (cross section A–A′) originating from a deeper sole thrust (not shown in the cross section) and terminating in the late Oligocene to early Miocene Pysht Formation (unit MΦm$_p$). This interpretation supports structural evidence from nearby Ennis Creek and is typical of structural geometries applied in other parts of the accretionary prism on the Olympic Peninsula (Gerstel and Lingley, 2000; Lingley, 1995). MacLeod and others (1977) noted the possible existence of this fault based on geophysical data. In this study, we refer to the segment that crosses the field area as the Lower Elwha fault, in keeping with the informal naming used by Atkins and others (2003). Brown (1970) referred to a part of the same structure as the Freshwater fault, which was also shown on Brown and others' (1960) geologic map, but was not named. We show this fault as a single, inferred, concealed fault on the map, because of some uncertainty as to its exact location and the extent of imbrication. Brown and others (1960) and Brown (1970) showed the southern side of the fault (where they mapped it in the adjacent Elwha and Angeles Point quadrangles) as upthrown, but we agree with Dragovich and others (2002) and Schasse (2003) who show the north side as upthrown.

The second previously mapped fault trends along the Lake Creek and Little River valleys. It was mapped in the east half of the quadrangle as the Lake Creek fault (Brown and others, 1960; Brown, 1970), but Tabor and Cady (1978) connect it to the Boundary Creek fault of Brown and others (1960) and Brown (1970) west of the map area. Brown (1961) speculated on the connection but did not show it on his 1970 map. We refer to this fault as the Lake Creek–Boundary Creek fault (**LCBCF**). The lidar-based DEM of the field area reveals surface scarps that cut JFL glacial drift (scarps shown by a solid line) coincident with the LCBCF in the Little River and Lake Creek valleys, indicating that this fault may have been active after about 13.3 ka (Fig. 1; Polenz and others, 2004). Field evidence indicates a south-side-down relationship for this fault. We also mapped a 0.8-mi-long surface scarp expressed on lidar near the western edge of the map as a fault that splays off the LCBCF to the northeast. Field inspection of the scarp indicates that the fault is north-side down.

The LCBCF offsets late Eocene and older units, but little is known about the timing of its activity. The lidar data document evidence of minor Quaternary movement. Scarps on unit Qgd surfaces in the field area suggest postglacial fault activity. Polenz and others (2004) speculate on possible age constraints based on their observations of field relations around the Elwha River and Indian Creek.

Two inferred transverse faults with northeast and northwest strikes that cut regional structural trends, originally mapped by Brown and others (1960) and later modified by Brown (1970), are shown on our map. The most easterly of these two faults, the Ennis Creek fault (Brown, 1970), strikes northeast and was inferred by Brown (1970) to account for anomalies between the bedding attitudes and lithologic characteristics of bedrock exposures in the uplands and the exposures along strike in the bed of Ennis Creek. Both faults are inferred, apparently to explain the abrupt juxtaposition of basaltic rocks of the Crescent Formation with siltstones of the Aldwell Formation and marine sediments within the Crescent Formation. These two faults together form a graben between them. We have applied modifications to these faults where our field evidence seemed to warrant a change.

We modified the geology along Ennis Creek near the headwaters of Lees Creek (adjacent to cross section A–A′) in order to resolve a volumetric problem presented by the geology as mapped by Brown (1970). More specifically, more than 50 percent of the Makah Formation (unit ΦEm$_m$) was missing between Morse Creek, 2 mi east of the map area, and Ennis Creek. Although our interpretations are equivocal, we believe the original mappers had misidentified siltstones of the Hoko River Formation (unit Em$_{2h}$) exposed in Ennis Creek as Aldwell Formation (unit Em$_{2a}$). Previous interpretations required a major structural culmination in this area for which we have no supporting data, except questionable fossil assemblages. Therefore we use the simpler interpretation shown on the map.

We show a third northeast-trending inferred transverse fault, mapped by Tabor and Cady (1978), that juxtaposes marine sedimentary and basaltic rocks of the Crescent Formation just west of Heather Park. We have no information on movement of the fault, except for the juxtaposed contrasting rock types. We show two other northeast-trending faults, also mapped by Tabor and Cady (1978), extending into the map area from the south, with Crescent Formation on both sides of the faults.

DESCRIPTIONS OF MAP UNITS

HOLOCENE NONGLACIAL DEPOSITS

Qf — **Fill (recent)—**Clay, silt, sand, gravel, organic matter, riprap, and debris emplaced to elevate and reshape the land surface; includes engineered and non-engineered fills; shown only where fill placement is relatively extensive, sufficiently thick to be of geotechnical significance, and readily verifiable.

Qml — **Modified land (recent)—**Soil, sediment, or other geologic material locally reworked by excavation and (or) redistribution to modify topography; includes mappable sand and gravel pits excavated mostly into unit Qgo$_i$.

Qb — **Beach deposits (Holocene)—**Sand and cobbles, may include silt, pebbles, and boulders; usually a mix with variable proportions of northern and Olympic rocks; pebble-size and larger clasts typically well rounded and flat; locally well sorted; loose.

Qa, **Qa$_f$** — **Alluvium (early Holocene–recent)—**Gravel, sand, silt, clay, and peat; variably sorted; loose; bedded; deposited in stream beds and estuaries and on flood plains; may include lacustrine and beach deposits; mostly of Olympic derivation, but may contain northern clasts (typically <10%). Unit Qa may locally interfinger with unit Qgo and grade down into units Qoa and Qgo in drainage basin segments not at grade with MSL (for an example, see Petersen and others, 1983). Subscript 'f' indicates an alluvial fan.

Qp — **Peat and marsh deposits (Holocene)—**Organic and organic-matter-rich mineral sediments deposited in closed depressions; includes peat, muck, silt, and clay in and adjacent to wetlands.

Qmw — **Mass wasting deposits (Holocene)—**Boulders, gravel, sand, silt, and clay; generally unsorted but may be locally stratified; typically loose; shown along mostly colluvium-covered slopes that appear potentially unstable; contains exposures of underlying units and landslides that we either could not map with confidence or are too small to show as separate features.

Qls — **Landslide deposits (Holocene)—**Boulders, gravel, sand, silt, and clay in slide body and toe; underlying units make up the head scarps (however, landslides as mapped include the headscarp); mapped primarily from lidar imagery; angular to rounded; unsorted; generally loose, unstratified, broken, and chaotic, but may locally retain primary bedding structure; commonly includes liquefaction features; deposited by mass wasting processes other than soil creep and frost heave; typically in unconformable contact with surrounding units. Unit includes inactive slides. Some slides are too small to show at map scale, and many unstable slopes lack definite landslide characteristics. Thus, absence of a mapped landslide does not imply absence of hazard. All steep slopes are potentially unstable, and a site-specific geotechnical evaluation is advisable for construction there. The Pysht Formation (unit MΦm$_p$), the Aldwell Formation (unit Em$_{2a}$), marine sedimentary rocks of the Crescent Formation (unit Em$_{1c}$), and Quaternary units are particularly susceptible to landslide activity.

Qoa, **Qoa$_f$** — **Older alluvium (Pleistocene–early Holocene)—**Gravel, sand, silt, clay, and peat; variably sorted; loose; generally bedded and permeable; unit Qoa deposited in stream beds and estuaries, and on flood plains; may include some lacustrine and beach deposits. Unit Qoa$_f$ deposited as fans; locally grades down into or interfingers with unit Qgo; may also locally grade up into unit Qa. Unit Qoa deposits form terraces up to 200 ft above modern valley floors. The highest terraces grade to late-Wisconsinan glaciomarine drift deposits included in unit Qgo$_s$. Unit Qoa may record a relative sea level rise due to deglaciation. Deposition of unit Qoa is thought to have ended in most areas once streams incised into the coastal plain in response to relative sea level lowering that accompanied post-glacial crustal rebound (Fig. 1).

LATE WISCONSINAN GLACIAL DEPOSITS

Qgo, **Qgo$_s$**, **Qgo$_i$** — **Recessional outwash and glaciomarine drift (Pleistocene)—**Gravel, sand, silt, clay, and locally peat; characterized by northern rock types; typically well rounded; loose; generally well sorted; mostly stratified; deposited by glacial meltwater as opposed to nonglacial streams; locally grades up into or interfingers with post-glacial alluvium (units Qoa and Qa). Glaciomarine drift facies includes pebbly silt and clay and discontinuous layers of silty sand and is weakly stratified to nonstratified. Glaciomarine deposits (included with unit Qgo$_s$ in the northern part of the map area) are deposited to a minimum level of approximately 130 ft (Dethier and others, 1995, fig. 3). Several subtle topographic steps that roughly parallel the shoreline on the coastal plain may include additional older, higher, post-glacial shoreline berms; unit Qgo is generally stratigraphically beneath, but partially coeval with unit Qoa, and deposition of unit Qgo may locally have continued thousands of years after deposition of unit Qoa ceased (Fig. 1; Polenz and others, 2004; Heusser, 1973). Units Qgo and Qoa are typically difficult to distinguish from each other. Deposition of unit Qgo began as ice receded some time between 14,460 ±200 ^{14}C yr B.P. and 12,000 ±310 ^{14}C yr B.P. (Heusser, 1973; Petersen and others, 1983) and may locally have continued until after 8 ^{14}C ky (Heusser, 1973). Deposition of the glaciomarine drift facies occurred at or about 12,600 ± 200 ^{14}C yr B.P. (Dethier and others, 1995; Fig. 1). The glaciomarine facies of unit Qgo is the lithostratigraphic equivalent of Everson Glaciomarine Drift in the Puget Lowland. Subscript 's' indicates sand or finer-grained facies. Subscript 'i' indicates outwash interpreted as ice-contact deposits, which are characterized by hummocky topography and ice-collapse features and are mined for their sand and gravel resource.

Qgt — **Juan de Fuca lobe till (Pleistocene)—**Unsorted and highly compacted mixture of clay, silt, sand, gravel, and boulders deposited directly by glacier ice; gray where fresh and light yellowish brown where oxidized; permeability very low where lodgement till is well developed; clasts are northern source but with abundant Olympic rock types where Olympic sediments are abundant in the substrate; most commonly matrix supported but locally clast supported; matrix more angular than water-worked sediments; cobbles and boulders commonly faceted and (or) striated; forms a patchy cover ranging from <0.5 ft to 20 ft thick; thicknesses of 2 to 10 ft are most common; may include outwash clay, sand, silt, and gravel, or loose ablation till that is too thin to substantially mask the underlying, rolling till plain; erratic boulders commonly signal that this unit is underfoot, but such boulders may also occur as lag deposits where the underlying deposits have been modified by meltwater; typically, weakly developed modern soil has formed on the cap of loose gravel, but the underlying till is unweathered; local textural features include flow banding. Unit Qgt may be overlain by unit Qgo and underlain by unit Qga or other older units. Unit Qgt may include local exposures of older till that are indistinguishable in stratigraphic position, lithology, and appearance.

Qgl — **Glaciolacustrine sediment (Pleistocene)—**Stratified, well-sorted sand, silt, or clay with local dropstones of northern provenance; brown to gray; may be massive, laminated, varved, or otherwise stratified; ranges from loose to compact; most exposures are stiff; includes advance and recessional lake deposits. Unit most commonly exposed along stream cutbanks, such that few surfaces are mapped as unit Qgl.

Qga, **Qga$_s$** — **Advance outwash (Pleistocene)—**Sand and sandy pebble to cobble gravel; local silts and clays; may contain till fragments; dominated in most exposures by northern sediment; compact; gray to grayish brown and grayish orange; clasts well rounded; well sorted; parallel-bedded, locally cross-bedded; most exposures suggest a unit thickness of <20 ft. Unit Qga is commonly overlain by unit Qgt along a sharp contact and is stratigraphically above unit Qu$_p$. The age of unit Qga in the project area is suggested by radiocarbon ages of "18,265 ±345" and "17,350 ±1260" reported by Blunt and others (1987) from bluff exposures at Port Williams, 14 mi to the east. Subscript 's' indicates that deposits are dominantly sand-sized or finer. We interpret our mapped exposures of unit Qga$_s$ as glaciolacustrine. They may contain dropstones and are characterized by planar laminations but locally include cross-bedding and soft-sediment deformation features.

Qad — **Undifferentiated alpine drift (Pleistocene)—**Till, outwash, morainal deposits, minor talus, and other sediments of Olympic source; lacks age control but is thought to pre-date arrival of the late Wisconsinan JFL ice.

Qgd — **Juan de Fuca lobe drift, undivided (Pleistocene)—**Till (may include flow-till and ablation till), advance and recessional outwash sand and gravel, and glaciolacustrine and glaciomarine sand, silt, and clay; generally of northern source, but may locally include Olympic-source drift; used for materials not differentiable at map scale into units Qgo, Qgl, Qgt, or Qga due to poor exposure and poor access. The age range of unit Qgd is that of the included units (~12–19 ka), but may include local exposures of older drift that resemble late Wisconsinan drift in stratigraphic position, lithology, and appearance.

UNDIFFERENTIATED HOLOCENE AND PLEISTOCENE DEPOSITS

Qu — **Undifferentiated glacial and nonglacial deposits (Holocene and Pleistocene)—**Includes units Qgt, Qoa, and Qoa$_f$; shown only in cross section A–A′ where scale doesn't allow for subdivision.

PLEISTOCENE DEPOSITS OLDER THAN JUAN DE FUCA LOBE TILL

Qu$_p$ — **Undifferentiated pre-late Wisconsinan sediments (Pleistocene)—**Gravel, sand, silt, clay, peat, and till; variably sorted; mostly bedded; compact; apparent maximum thickness of ~200 ft; contains both northern and Olympic glacial and nonglacial deposits. Radiocarbon analysis of wood fragments obtained from a sand facies 78 ft below the ground surface in a water well 3.5 mi west of the map area yielded a date of 37,800 ± 1100 ^{14}C yr B.P. (Polenz and others, 2004) suggesting that much of the unit consists of deposits of the marine oxygen isotope stage 3 (70–15 ka). Shoreline exposures may laterally grade into unit Qoa$_p$ to the west of the map area (Polenz and others, 2004), suggesting that an ancestral Elwha River may have carried sediment several miles further east than the modern Elwha. A peat sample collected near sea level from the shoreline bluff at the west end of Ediz Hook yielded a radiocarbon date of >44,620 yr B.P. (Beta No. 123218), suggesting an age correlative to marine oxygen isotope stage 3 or older for the lower part of that section. The northern-source sediments within the unit are undated but are included in the unit because local stratigraphic relations suggest that they mostly reflect pre-late Wisconsinan glaciation(s) (marine oxygen isotope stage 4 or earlier).

TERTIARY SEDIMENTARY AND VOLCANIC ROCKS

TWIN RIVER GROUP—Divided into:

MΦm$_p$ — **Pysht Formation (Miocene–Oligocene)—**Marine mudstone, claystone, and sandy siltstone; also contains 1- to 20-ft-thick beds of calcareous sandstone; unweathered mudstone, claystone, and siltstone are medium gray to dark greenish gray; weathers pale yellowish brown to medium brown; massive, poorly indurated; mudstone may contain thin beds of calcareous claystone; argillaceous rocks contain sparsely disseminated calcareous concretions; mollusk shell fragments, foraminifera, and carbonized plant material are common in mudstone; gradational with the underlying Makah Formation (unit ΦEm$_m$) (Snavely and others, 1978). The thickness of the unit was not precisely determined in the Port Angeles area because of poor exposure, but is assumed to be ~1000 ft from a cross section by Brown and others (1960) along Morse Creek, 1 mi east of the Port Angeles quadrangle. In the Port Angeles quadrangle, the unit is restricted to local structural depressions along the Clallam syncline where the lowest strata in the formation are preserved. Unit is highly susceptible to landsliding; contains lower Saucesian and upper Zemorrian foraminifera (Rau, 1964, 1981, 2000, 2002); mollusks are indicative of the Juanian Stage (Addicott, 1976, 1981).

ΦEm$_m$ — **Makah Formation (Oligocene–Eocene)—**Marine siltstone, mudstone, and minor thin-bedded sandstone; greenish gray to olive-brown, weathers to grayish orange and yellowish brown; dark gray to black where carbonaceous; massive to thin- and rhythmically bedded; spherical calcareous concretions (often containing fossil shells and plants) and nodules occur throughout; sandstone is angular, very fine to medium grained, subquartzose, and feldspatholithic; approximately 5100 ft thick at Morse Creek 1 mi east of the Port Angeles quadrangle (Brown and others, 1960); crops out on the south limb of the Clallam syncline and is tentatively identified north of the synclinal axis in two exposures along Tumwater and Valley Creeks; gradational with the more arenaceous rocks of the underlying Hoko River Formation (unit Em$_{2h}$) (Snavely and others, 1978); contains upper Narizian and Refugian foraminifera (Rau, 1964, 2000, 2002).

Em$_{2h}$ — **Hoko River Formation (upper Eocene)—**Marine lithofeldspathic sandstone and siltstone in equal amounts, with pebble–cobble conglomerate lenses and laterally and vertically gradational contacts; thick beds of sandstone and pebble-cobble conglomerate occur locally near the base of unit in exposures at Mount Pleasant where the lower 1500 ft of section is exposed (cross section A–A′); sandstone is gray to olive-gray, fine to very coarse grained to granular, well bedded and thin to very thick bedded; siltstone contains thin beds and laminae of very fine grained sandstone, is well bedded, well indurated, locally cemented with calcium carbonate, and may contain calcareous concretions. Thickness variations north of The Foothills are probably due to thinning of unit Em$_{2h}$ near structural highs of older rocks; conformable with the Aldwell Formation (unit Em$_{2a}$) in The Foothills and at Mount Pleasant where the absence of the Lyre Formation is due to transgressive overlap by younger sedimentary rocks (Brown and others, 1960); contains upper Narizian foraminifera (Snavely and others, 1980; Rau, 2000).

TERTIARY SEDIMENTARY AND VOLCANIC ROCKS OLDER THAN THE TWIN RIVER GROUP

Em$_{2a}$ — **Aldwell Formation (middle Eocene)—**Marine siltstone and sandy siltstone with sparse interbeds of fine- to very fine grained feldspatholithic sandstone. Siltstone is olive-gray to black and contains thin sandy laminations and local thin to medium beds of fine-grained limestone or calcareous very fine grained sandstone. Sandstone is greenish gray and weathers to brown and olive-gray; calcareous beds are distinguished by their tan weathered surfaces. Lenses of unsorted pebbles, cobbles, and boulders of basalt occur sporadically throughout the siltstone; pillow basalt, lenses of basalt breccia, and water-laid lapilli tuff (similar to unit Ev$_c$ of the underlying Crescent Formation) also occur throughout the siltstone; basaltic lenses occur near the base and midsection north of The Foothills (unit Evb$_a$). Unit Em$_{2a}$ is about 1500 ft thick at Mount Pleasant (cross section A–A′); susceptible to landslides, particularly where it crops out along steep slopes in the valley of Ennis Creek; and characterized by lower Narizian foraminifera, indicating a middle Eocene age (Armentrout and others, 1983; Rau, 1964). Divided into:

Evb$_a$ — **Basaltic rocks (middle Eocene)—**Basalt, conglomerate, breccia, and tuff similar to the Crescent Formation (unit Ev$_c$); consists of mappable pods north of The Foothills near the midsection of unit Em$_{2a}$; lenses and pods of rhyolitic rocks are mapped along with similarly occurring basaltic breccias in the Dry Hills within the Aldwell Formation (unit Em$_{2a}$) in the adjacent Elwha quadrangle (Polenz and others, 2004). A whole-rock analysis (Table 1, loc. 2) of a minor silicic component of unit Evb$_a$ north of The Foothills in the Port Angeles quadrangle appears to be a water-laid crystal-vitric rhyolitic tuffaceous siltstone.

Ev$_c$ — **Crescent Formation (middle and lower Eocene)—**Marine, tholeiitic, pillow-dominated basaltic rocks; includes minor aphyric basalt flows and minor gabbroic sills and dikes; may contain thin interbeds of basaltic tuff, chert, red argillite, limestone, siltstone, and abundant chlorite and zeolites; beds of marine sedimentary rocks are mapped as subunit Em$_{1c}$; dark gray to dark greenish gray, weathers to dark brown; massive basalt flows, basalt breccia, massive diabasic basalt, and volcaniclastic sandstone and conglomerate all grade into each other both laterally and vertically. Whole-rock XRF analyses are listed in Table 1. In the map area, the unit forms a belt from 3.5 to 5.5 mi wide. Reported ^{40}Ar/^{39}Ar plateau ages range from 45.4 Ma to 56.0 Ma (Babcock and others, 1994). The youngest age was from the base of unit Ev$_c$ causing Babcock and others (1994) to suggest that the basalts may be part of separate extrusive centers. Contains foraminiferal assemblages referable to the Penutian to Ulatisian Stages (Rau, 1964). Divided into:

Em$_{1c}$ — **Marine sedimentary rocks (middle and lower Eocene)—**Siltstone, basaltic flow breccia, tuff breccia, volcanic conglomerate, and volcanolithic sandstone, less abundant chert and calcareous argillite; gray, green, red, or black; clasts chiefly basalt and diabase; lithic, calcareous, and fossiliferous; breccias, tuffs, and sandstones are normally graded; sedimentary rocks well stratified; susceptible to landsliding on steep slopes. Unit Ev$_c$ occurs as isolated lenses within unit Em$_{1c}$, is several hundreds of feet thick where exposed along north-facing slopes of The Foothills, and is inferred to be present in the subsurface beneath JFL drift in the valleys of Lake Creek and Little River (based on water-well drillers logs and small exposures of the unit scattered throughout the glacial drift covered area) (see cross section A–A′). A whole-rock XRF analysis of a small lens or pod of a volcanic flow within unit Em$_{1c}$ along the Hurricane Ridge road, produced basalt chemistry (Table 1, loc. 3). Foraminifera from unit Em$_{1c}$ range in age from Penutian to Ulatisian (Rau, 1981, 2000).

GEOLOGIC SYMBOLS

- Contact—dashed where approximately located, dotted where concealed
- High-angle dip-slip fault—question mark where queried, dashed where approximately located, dotted where concealed
- Thrust fault, sawteeth on upper plate—long dashed where approximately located, short dashed where inferred, dotted where concealed
- Fault of unknown displacement, inferred
- Syncline—dashed where approximately located, dotted where concealed
- Bearing of minor syncline; plunge added when known
- Bearing of minor anticline; plunge added when known
- Landslide scarp, hachures on downslope side
- Direction of landslide movement
- Strike and dip of beds
- Strike and dip of overturned beds
- Strike of vertical beds, dot indicates top of beds
- Southern limit of late Wisconsinan continental glaciation, hachures toward ice
- Radiocarbon age-date sample locality
- Geochemistry sample locality

ACKNOWLEDGMENTS

This map was concurrently mapped with the Elwha and Angeles Point quadrangles and was produced in cooperation with the U.S. Geological Survey National Cooperative Geologic Mapping Program, Agreement Number 03HQAG0086, which partially supported our mapping project. We thank Tom Schindler (Clallam County Department of Community Development) for providing County GIS resources and site-specific information and Randy Johnson and Ernie Latson (Green Crow Timber Co.) for access to Green Crow timberlands. We also thank Olympic National Park Service for allowing us to map within the National Park boundaries. Thanks also to Bill Lingley, Division of Geology and Earth Resources, for a technical review and helpful advice regarding cross section development. Last, but not least, thanks to the uncounted people who permitted us to study geologic exposures on their land and provided site-specific records and local knowledge.

REFERENCES CITED

Addicott, W. O., 1976, Neogene molluscan stages of Oregon and Washington. *In* Fritsche, A. E.; Ter Best, Harry, Jr.; Wornardt, W. W., editors, The Neogene symposium—Selected technical papers on paleontology, sedimentology, petrology, tectonics and geologic history of the Pacific coast of North America: Society of Economic Paleontologists and Mineralogists Pacific Section, 51st Annual Meeting, p. 95-115.

Addicott, W. O., 1981, Significance of pectinids in Tertiary biochronology of the Pacific Northwest. *In* Armentrout, J. M., editor, Pacific Northwest Cenozoic biostratigraphy: Geological Society of America Special Paper 184, p. 17-37.

Armentrout, J. M.; Hull, D. A.; Beaulieu, J. D.; Rau, W. W., coordinators, 1983, Correlation of Cenozoic stratigraphic units of western Oregon and Washington; Draft: Oregon Department of Geology and Mineral Industries Open-File Report O-83-5, 268 p., 1 pl.

Atkins, V. D.; Molinari, M. P.; Burk, R. L., 2003, Quaternary Geology of the lower Elwha River Valley, Washington [abstract]: Geological Society of America Abstracts with Programs, v. 35, no. 6, p. 80.

Babcock, R. S.; Suczek, C. A.; Engebretson, D. C., 1994, The Crescent "terrane", Olympic Peninsula and southern Vancouver Island. *In* Lasmanis, Raymond; Cheney, E. S., convenors, Regional geology of Washington State: Washington Division of Geology and Earth Resources Bulletin 80, p. 141-157.

Blunt, D. J.; Easterbrook, D. J.; Rutter, N. W., 1987, Chronology of Pleistocene sediments in the Puget Lowland, Washington. *In* Schuster, J. E., editor, Selected papers on the geology of Washington: Washington Division of Geology and Earth Resources Bulletin 77, p. 321-353.

Booth, D. B., 1987, Timing and processes of deglaciation along the southern margin of the Cordilleran ice sheet. *In* Ruddiman, W. F.; Wright, H. E., Jr., editors, North America and adjacent oceans during the last glaciation: Geological Society of America DNAG Geology of North America, v. K-3, p. 71-90.

Brown, R. D., Jr., 1961, Geology of the north central Olympic Peninsula, Washington: U.S. Geological Survey unpublished manuscript, 1 v.

Brown, R. D., Jr., 1970, Geologic map of the north-central part of the Olympic Peninsula, Washington: U.S. Geological Survey Open-File Report 70-43, 2 sheets, scale 1:62,500.

Brown, R. D., Jr.; Gower, H. D., 1958, Twin River Formation (redefinition), northern Olympic Peninsula, Washington: American Association of Petroleum Geologists Bulletin, v. 42, no. 10, p. 2492-2512.

Brown, R. D., Jr.; Gower, H. D.; Snavely, P. D., Jr., 1960, Geology of the Port Angeles–Lake Crescent area, Clallam County, Washington: U.S. Geological Survey Oil and Gas Investigations Map OM-203, 1 sheet, scale 1:62,500.

Clague, J.; Harper, J. R; Hebda, R. J.; Howes, D. E., 1982, Late Quaternary sea levels and crustal movements, coastal British Columbia: Canadian Journal of Earth Sciences, v. 19, no. 3, p. 597-618.

Dethier, D. P.; Pessl, Fred, Jr.; Keuler, R. F.; Balzarini, M. A.; Pevear, D. R., 1995, Late Wisconsinan glaciomarine deposition and isostatic rebound, northern Puget Lowland, Washington: Geological Society of America Bulletin, v. 107, no. 11, p. 1288-1303.

Dickinson, W. R., 1970, Interpreting detrital modes of greywacke and arkose: Journal of Sedimentary Petrology, v. 40, no. 2, p. 695-707.

Downing, J. P., 1983, The coast of Puget Sound—Its processes and development: University of Washington Press, 126 p.

Dragovich, J. D.; Logan, R. L.; Schasse, H. W.; Walsh, T. J.; Lingley, W. S., Jr.; Norman, D. K.; Gerstel, W. J.; Lapen, T. J.; Schuster, J. E.; Meyers, K. D., 2002, Geologic map of Washington—Northwest quadrant: Washington Division of Geology and Earth Resources Geologic Map GM-50, 3 sheets, scale 1:250,000, with 72 p. text.

Dragovich, J. D.; Pringle, P. T.; Walsh, T. J., 1994, Extent and geometry of the mid-Holocene Osceola mudflow in the Puget Lowland—Implications for Holocene sedimentation and paleogeography: Washington Geology, v. 22, no. 3, p. 3-26.

Galster, R. W., 1989, Ediz Hook—A case history of coastal erosion and mitigation. *In* Galster, R. W., chairman, Engineering geology in Washington: Washington Division of Geology and Earth Resources Bulletin 78, v. II, p. 1177-1186.

Gerstel, W. J.; Lingley, W. S., Jr., compilers, 2000, Geologic map of the Forks 1:100,000 quadrangle, Washington: Washington Division of Geology and Earth Resources Open File Report 2000-4, 36 p., 2 plates.

Heusser, C. J., 1973, Environmental sequence following the Fraser advance of the Juan de Fuca lobe, Washington: Quaternary Research, v. 3, no. 2, p. 284-306.

Johnson, D. M.; Hooper, P. R.; Conrey, R. M., 1999, XRF analysis of rocks and minerals for major and trace elements on a single low dilution Li-tetraborate fused bead: Advances in X-ray Analysis, v. 41, p. 843-867.

Lingley, W. S., Jr., 1995, Preliminary observations on marine stratigraphic sequences, central and western Olympic Peninsula, Washington: Washington Geology, v. 23, no. 2, p. 9-20.

Long, W. A., 1975, Salmon Springs and Vashon continental ice in the Olympic Mountains and relation of Vashon continental to Fraser Olympic ice. *In* Long, W. A., Glacial studies on the Olympic Peninsula: U.S. Forest Service, 1 v.

MacLeod, N. S.; Tiffin, D. L.; Snavely, P. D., Jr.; Currie, R. G., 1977, Geologic interpretation of magnetic and gravity anomalies in the Strait of Juan de Fuca, U.S.–Canada: Canadian Journal of Earth Sciences, v. 14, no. 2, p. 223-238.

Mathews, W. H.; Fyles, J. G.; Nasmith, H. W., 1970, Postglacial crustal movements in southwestern British Columbia and adjacent Washington State: Canadian Journal of Earth Sciences, v. 7, no. 2, part 2, p. 690-702.

Montanari, Alessandro; Drake, Robert; Bice, D. M.; Alvarez, Walter; Curtis, G. H.; Turrin, B. D.; DePaolo, D. J., 1985, Radiometric time scale for the upper Eocene and Oligocene based on K/Ar and Rb/Sr dating of volcanic biotites from the pelagic sequence of Gubbio, Italy: Geology, v. 13, no. 9, p. 596-599.

Mosher, D. C.; Hewitt, A. T., 2004, Late Quaternary deglaciation and sea-level history of eastern Juan de Fuca Strait, Cascadia: Quaternary International, v. 121, no. 1, p. 23-39.

Petersen, K. L.; Mehringer, P. J., Jr.; Gustafson, C. E., 1983, Late-glacial vegetation and climate at the Manis Mastodon site, Olympic Peninsula, Washington: Quaternary Research, v. 20, no. 2, p. 215-231.

Polenz, Michael; Wegmann, K. W.; Schasse, H. W., 2004, Geologic Map of the Elwha and Angeles Point 7.5-minute quadrangles, Clallam County, Washington: Washington Division of Geology and Earth Resources Open File Report 2004-14, 1 sheet, scale 1:24,000.

Rau, W. W., 1964, Foraminifera from the northern Olympic Peninsula, Washington: U.S. Geological Survey Professional Paper 374-G, 33 p., 7 pl.

Rau, W. W., 1981, Pacific Northwest Tertiary benthic foraminiferal biostratigraphic framework—An overview. *In* Armentrout, J. M., editor, Pacific Northwest Cenozoic biostratigraphy: Geological Society of America Special Paper 184, p. 67-84.

Rau, W. W., 2000, Appendix 4—Foraminifera from the Carlsborg 7.5-minute quadrangle, Washington. *In* Schasse, H. W.; Wegmann, K. W., Geologic map of the Carlsborg 7.5-minute quadrangle, Clallam County, Washington: Washington Division of Geology and Earth Resources Open File Report 2000-7, p. 24-26.

Rau, W. W., 2002, Appendix 3—Foraminifera from the Morse Creek quadrangle. *In* Schasse, H. W.; Polenz, Michael, Geologic map of the Morse Creek 7.5-minute quadrangle, Clallam County, Washington: Washington Division of Geology and Earth Resources Open File Report 2002-8, p. 16-17.

Salvador, Amos, 1985, Chronostratigraphic and geochronometric scales in COSUNA stratigraphic correlation charts of the United States: American Association of Petroleum Geologists Bulletin, v. 69, no. 2, p. 181-189.

Schasse, H. W., 2003, Geologic map of the Washington portion of the Port Angeles 1:100,000 quadrangle: Washington Division of Geology and Earth Resources Open File Report 2003-6, 1 sheet, scale 1:100,000.

Schasse, H. W.; Polenz, Michael, 2002, Geologic map of the Morse Creek 7.5-minute quadrangle, Clallam County, Washington: Washington Division of Geology and Earth Resources Open File Report 2002-8, 18 p., 2 plates.

Snavely, P. D., Jr.; Niem, A. R.; MacLeod, N. S.; Pearl, J. E.; Rau, W. W., 1980, Makah Formation—A deep-marginal-basin sequence of late Eocene and Oligocene age in the northwestern Olympic Peninsula, Washington: U.S. Geological Survey Professional Paper 1162-B, 28 p.

Snavely, P. D., Jr.; Niem, A. R.; Pearl, J. E., 1978, Twin River Group (upper Eocene to lower Miocene)—Defined to include the Hoko River, Makah, and Pysht Formations, Clallam County, Washington. *In* Sohl, N. F.; Wright, W. B., Changes in stratigraphic nomenclature by the U.S. Geological Survey, 1977: U.S. Geological Survey Bulletin 1457-A, p. 111-120.

Tabor, R. W.; Cady, W. M., 1978, Geologic map of the Olympic Peninsula, Washington: U.S. Geological Survey Miscellaneous Investigations Series Map I-994, 2 sheets, scale 1:125,000.

Zanettin, Bruno, 1984, Proposed new chemical classification of volcanic rocks: Episodes, v. 7, no. 4, p. 19-20. ■

Disclaimer: This product is provided 'as is' without warranty of any kind, either expressed or implied, including, but not limited to, the implied warranties of merchantability and fitness for a particular use. The Washington Department of Natural Resources will not be liable to the user of this product for any activity involving the product with respect to the following: (a) lost profits, lost savings, or any other consequential damages; (b) the fitness of the product for a particular purpose; or (c) use of the product or results obtained from use of the product. This product is considered to be exempt from the Geologist Licensing Act [RCW 18.220.190 (4)] because it is geological research conducted by the State of Washington, Department of Natural Resources, Division of Geology and Earth Resources.

Figure 1. Relative sea level and time line of events in the field area from the late Wisconsinan glaciation to the present. Post-glacial sea level curve mostly after Mosher and Hewitt (2004). Age control based on previously published radiocarbon dates. We used CALIB REV 4.4.2 software to convert (to ka) age estimates that were previously published in radiocarbon years. Upper axis is labeled in radiocarbon years before present (^{14}C yr B.P.) and is a nonlinear time scale. Lower axis is labeled in ka and is a linear time scale, within the limits of accuracy of radiocarbon data calibration.

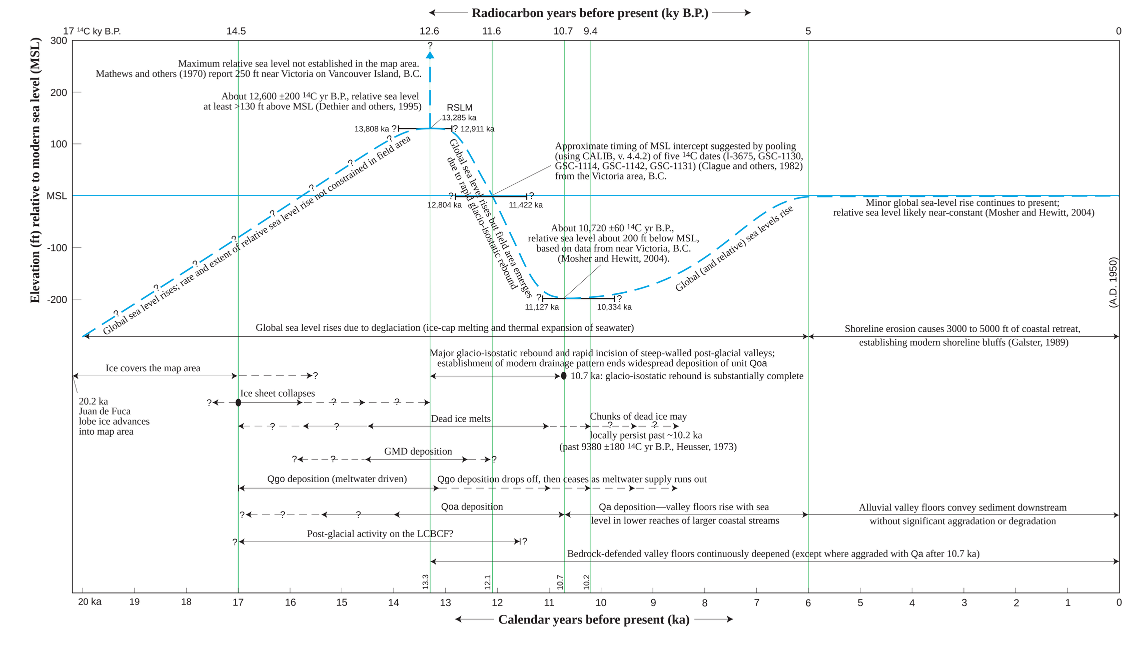

Table 1. Geochemical analyses for the Port Angeles quadrangle performed by x-ray fluorescence at the Washington State University GeoAnalytical Lab. Instrumental precision is described in detail in Johnson and others (1999). Major and trace elements normalized to 100 on a volatile-free basis, with total Fe expressed as FeO; LOI(%), percent loss on ignition

MAJOR ELEMENTS—NORMALIZED (weight percent)

Loc. no.	Sample no.	Geologic unit, rock type	Chemical analysis	SiO_2	TiO_2	Al_2O_3	FeO	MnO	MgO	CaO	Na_2O	K_2O	P_2O_5	Original total	LOI(%)
1	HS-59	Ev$_c$, basalt	basalt	47.02	2.334	14.73	14.58	0.225	6.62	10.12	3.73	0.26	0.236	97.54	– – –
2	HS-77	Evb$_a$, crystal-vitric tuffaceous siltstone	rhyolite	78.05	0.154	8.28	1.40	0.018	1.27	7.53	2.37	0.68	0.021	93.23	10.46
3	HS-86	Em$_{1c}$, invasive(?) basalt flow	basalt	47.08	2.339	14.16	13.28	0.283	6.21	13.40	2.70	0.14	0.241	96.96	– – –

TRACE ELEMENTS—NORMALIZED (parts per million)
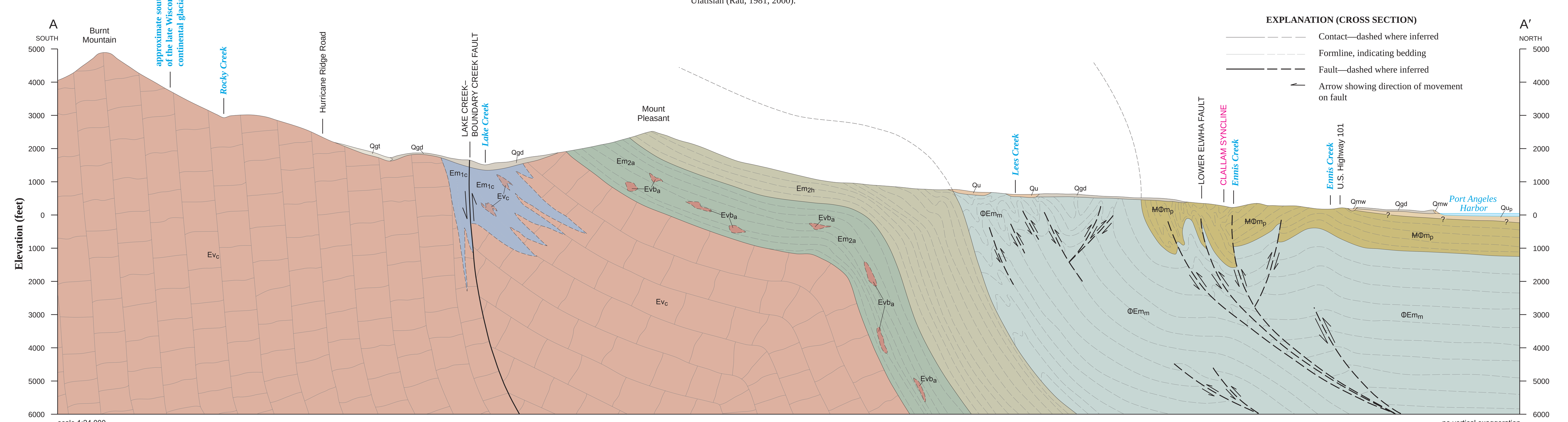
Loc. no.	Sample no.	Geologic unit, rock type	Chemical analysis	Ni	Cr	Sc	V	Ba	Rb	Sr	Zr	Y	Nb	Ga	Cu	Zn	Pb	La	Ce	Th
1	HS-59	Ev$_c$, basalt	basalt	53	85	45	445	52	6	273	153	44	12.6	20	247	119	1	8	25	1
2	HS-77	Evb$_a$, crystal-vitric tuffaceous siltstone	rhyolite	7	6	4	7	644	19	689	402	102	38.4	9	21	105	70	30	71	3
3	HS-86	Em$_{1c}$, invasive(?) basalt flow	basalt	53	88	45	449	130	4	215	161	46	13.3	22	230	151	6	7	30	1